Structural, electrical, and optical properties of a-$Si_{1-x}Ge_x$:H and an inferred electronic band structure

K. D. Mackenzie, J. R. Eggert, D. J. Leopold, Y. M. Li, S. Lin,* and William Paul
Division of Applied Sciences, Harvard University, Cambridge, Massachusetts 02138
(Received 21 September 1984)

Amorphous hydrogenated silicon-germanium alloys have been prepared over the full composition range by rf glow discharge of silane-germane mixtures at substrate temperatures between 200 °C and 400 °C. A detailed description of the deposition apparatus, preparation procedures, and techniques of property measurement is given. The dependences on substrate temperature and germanium content of the optical-absorption, photoconductivity, and photoluminescence spectra and of the conductivity-temperature relation are reported and analyzed. Electronic band structures (density of states versus energy) are proposed which incorporate the changes in the optical energy gap with composition and the energies of the dangling-bond states on germanium and silicon atoms. The observed properties are examined in detail in relation to the proposed new density-of-states structure. The possibility is explored of explaining the poor photoelectronic properties with and without invoking a higher density of defects in the alloys. The occurrence of a two-phase heterostructure and the possibility of changes in its constitution, especially the location in it of the hydrogen, with changing substrate temperature and film composition are also discussed.

I. INTRODUCTION

Hydrogenated amorphous silicon-based binary alloys are currently a subject of much interest in the development of high-efficiency photovoltaic solar cells.[1–4] By alloying a-Si:H with such elements as Ge or Sn, it is possible to narrow the band gap and thus improve the long-wavelength response. It appears that independent of the preparation method, rf sputtering,[5,6] cathodic sputtering,[7] dc glow discharge,[8,9] or rf glow discharge,[1–3,10–12] alloying Si with Ge leads to a deterioration of the photoelectronic properties. Such behavior is not peculiar to a-$Si_{1-x}Ge_x$:H alloys or indeed narrow band-gap alloys. Similar findings have been reported for other alloy systems such as a-$Si_{1-x}C_x$:H[13,14] and a-$Si_{1-x}Sn_x$:H.[15,16] At the time of writing, no solar cell utilizing a hydrogenated amorphous silicon-based binary alloy has a better efficiency than the best cells using a-Si:H. Indeed, no tandem solar cell incorporating such an alloy has a better efficiency than unalloyed nontandem solar cells. Paul and coworkers have already reported on the optical, electrical, and structural properties of a-$Si_{1-x}Ge_x$:H alloys prepared by dc glow discharge[8,9,17–19] and rf sputtering.[5,19,20] Some results have also been reported on unhydrogenated a-$Si_{1-x}Ge_x$ produced by the latter method.[5] From the study of the dc glow discharge material, it was deduced that, normalized to the Si/Ge ratio, more H is bonded to the Si atoms than to the Ge.[8,9,17,18] (Similar findings have been recently reported for rf sputtered[6] and rf glow discharge[21] a-$Si_{1-x}Ge_x$:H.) It is therefore possible that Ge may be left with an associated higher density of (dangling-bond) defect states. Indeed, the ESR measurements of Morimoto *et al.*[21] indicate that the ratio of Ge dangling bonds to Ge atoms increases drastically with increasing x. However, it appears unlikely that this is the root cause of the inferior properties; work of von Roedern *et al.*[9] showed that the magnitudes of the photoconductivity and the photoluminescence (PL) are much larger than would be expected on this basis. (Recent work of Rudder *et al.*[22] using dual magnetron sputtering shows that the H attachment ratio can be normalized by varying the deposition conditions.) Another explanation has been put forward to explain the inferior properties. Paul *et al.*[8,9,17,18] inferred from hydrogen evolution experiments the existence of weakly bonded hydrogen in a-Ge:H and in a-$Si_{1-x}Ge_x$:H alloys containing a high Ge content. This suggested that the weakly bonded hydrogen could perturb the film structure resulting in heterostructure. The nature of the heterostructure may be responsible for the observed properties.

The present report concerns an investigation of the optical, electrical, and structural properties of a-$Si_{1-x}Ge_x$:H prepared by the rf glow discharge technique. Earlier work of this group[20] on the determination of the midgap density of states as a function of optical gap showed that for the same value of optical gap, sputtered a-$Si_{0.7}Ge_{0.3}$:H has a lower state density than sputtered unalloyed a-Si:H of different (lower) H content, and, again for the same optical gap, glow discharge a-Si:H has lower state density than sputtered a-Si:H. From this, it may be inferred that *glow discharge* a-$Si_{1-x}Ge_x$:H will possess a lower state density than *sputtered* a-$Si_{1-x}Ge_x$:H for the same optical gap. Thus, the present investigation is concerned with the properties of rf glow discharge a-$Si_{0.5}Ge_{0.5}$:H alloys as a function of substrate temperature and of a-$Si_{1-x}Ge_x$:H as a function of Ge content. All of the specimens were prepared in a deposition unit[23] which is capable of producing device grade a-Si:H as evidenced, for example, by the low density of midgap states [$\sim 3\times 10^{15}$ $cm^{-3}eV^{-1}$ by the space-charge-limited-current (SCLC) technique][24] and the high sensitivity of the conductivity activation energy,[25] subband-gap absorption,[24] $\mu\tau$ products,[25] and photo-

conductivity[24] to low levels (ppm range) of phosphorus doping. Care has been taken to eliminate or considerably reduce any known sources of impurities.

From correlations made between the optical, electrical, and structural properties new information is obtained about the alloys. A band structure for the $x=0.5$ alloy is suggested, which takes account of the different energies of electrons in Ge and Si dangling-bond states and of the shifts in the conduction- and valence-band edges with alloying. This new band structure is capable of rationalizing several of the observed photoelectronic properties, without requiring as large an increase in defect density as formerly for the best a-Si:H. The structural measurements support our earlier suggestion of increased heterostructure in the alloys, which implies that full understanding of the electrical and optical properties must eventually involve a more complete analysis of the band structures of both island and tissue material.

II. EXPERIMENTAL DETAILS

In this section, details are given of our sample preparation and other experimental techniques.

A. Sample preparation

All of the samples were prepared as thin films by the rf glow-discharge decomposition of silane-germane mixtures. Figure 1 illustrates the main features of our deposition system.[23] A major consideration in the design of the system was the elimination or reduction of contamination from sources such as water vapor and oxygen that can result in inferior film properties.[26–28] Thus, the use of stainless-steel gas-feed lines which were short, a choice where possible of stainless-steel components in the deposition chamber, the baking of all stainless-steel parts including the joints, and the use of a turbomolecular pump capable of producing a high base vacuum were considered essential to reduce contamination to an acceptable level. As shown in Fig. 1, the deposition takes place within a plasma reactor that fits as an insert in an ultrahigh-vacuum (UHV) chamber. The plasma is confined to the reactor away from surfaces that could be sputtered. The majority of components of the reactor and the chamber are made from stainless steel and all joints are sealed by Cu gaskets. The short gas-feed lines to the system, the reactor, the joints, and the walls of the chamber are all bakeable. The reactor can be baked to a temperature of 350—400 °C. The system is evacuated by a turbomolecular pump which is backed by a rotary pump. Prior to deposition, after overnight bakeout, the base pressure is 3×10^{-8} Torr or better. During deposition, a residual gas analyzer (RGA)[29] is used to monitor for impurities in the chamber. A qualitative analysis indicated that the main impurities detected, H_2O and CO_2, are present relative to the highest peak in the RGA spectrum ($m/e=30$, the main peak of SiH_4) in levels of 50 and 150 ppm, respectively. During deposition, with the main gate valve closed, the chamber is pumped via the throttle valve by the turbomolecular pump. The desired pressure in the chamber is set on a pressure controller unit which is electrically interfaced with the baratron pressure gauge and

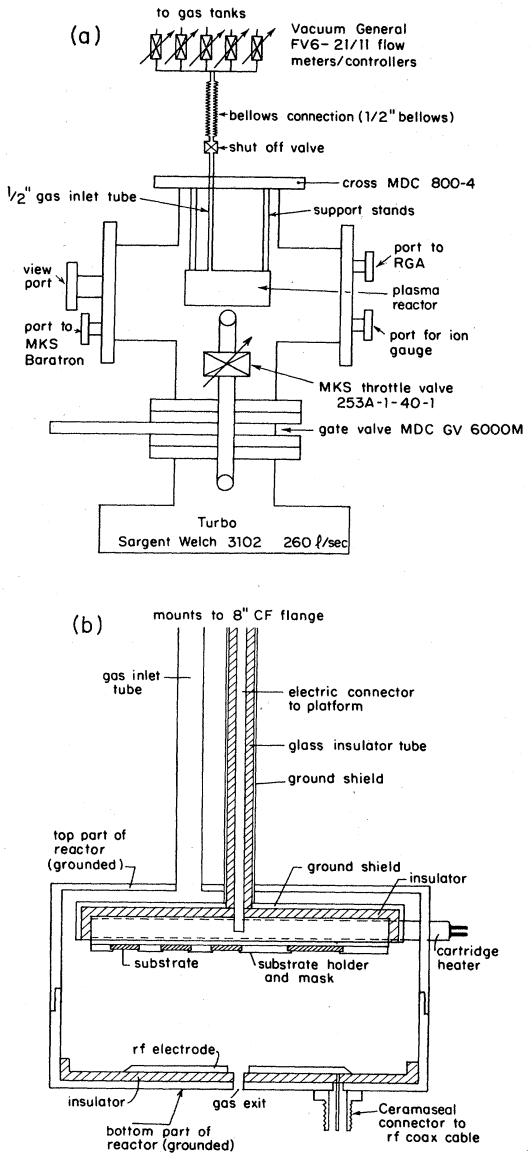

FIG. 1. (a) Schematic of the rf glow discharge deposition system. (b) Details of the plasma reactor.

the throttle valve. In the reactor, the substrates are mounted upside down (to reduce pinhole problems associated with dust) on a heated ungrounded (floating) electrode. The thermocouple used to measure the substrate temperature is embedded in the copper heater block on which the heated electrode is mounted. The SiH_4 and GeH_4 gases are admitted via separate electronic flow controllers into a short common mixing manifold before entering the reactor. The gas mixture flows radially inward between the heated electrode and the rf electrode below. The electrode configuration is asymmetric; the heated electrode is the larger and is 10 cm in diameter. As a matter of safety, the exhaust gases are diluted with nitrogen gas after the turbo pump then passed via the rotary pump into a furnace where they are decomposed at a temperature of about 800 °C. The furnace is vented out-

side the laboratory. An oil filtering system on the rotary pump is used to remove the particulates created by the reaction of the gases and the hydrocarbon pump oil. The furnace and filtering system, together with the rotary pump, are enclosed in a fume cabinet while the toxic gases are located in a separate cabinet. The SiH_4 and GeH_4 gases are supplied by Matheson and both are 99.99% pure. Contamination, sometimes severe, of SiH_4 with chlorosilanes, has been reported by Corderman and Vanier.[30] However, RGA analysis shows no chlorosilanes in excess of the ppm level in the gases we have used.

All of the specimens were prepared at a frequency of 13.56 MHz. For the alloys, the chamber pressure was held constant at 0.25 Torr and the net rf power at 3 W. The a-$Si_{0.5}Ge_{0.5}$:H alloys were prepared at various substrate temperatures covering the range 230 to 372 °C. The SiH_4 and GeH_4 flow rates were kept fixed at 12 cm^3 at STP per minute (SCCM) and 3 SCCM, respectively. For this series of specimens, the average Ge content was 52 ± 1 at. % as determined by electron microprobe. No correlation was found between Ge content and substrate temperature T_s. Films of a-$Si_{1-x}Ge_x$:H with x values ranging from 0.14 to 0.74 were grown at 300 °C. The SiH_4 flow rate was kept at 12 SCCM and the GeH_4 flow rate varied from 0.48 to 6.17 SCCM. The unalloyed a-Si:H films were prepared at a net rf power of 4 W, T_s of 230 °C, pressure of 0.20 Torr, and SiH_4 flow rate of 20 SCCM; these are the conditions that give films of suitable quality for device applications. The unalloyed a-Ge:H specimens were prepared at a net rf power of 3 W, T_s of 260 °C, pressure of 0.25 Torr, and GeH_4 flow rate of 10 SCCM. Deposition rates were between 80 and 200 Å min^{-1} and the specimen thicknesses ranged from 1 to 11 μm. In each run, films were co-deposited on a selection of different substrates necessary for the different types of experiments described below. In all cases, the substrates, excluding the fragile microgrids used for electron microscopy, were ultrasonically cleaned in baths of trichloroethylene, acetone, and methanol and then dried with N_2 gas before loading into the system.

Over 40 sets of films have been prepared for this work under the variety of deposition conditions described below. Good run-to-run reproducibility of the measured properties has been found for specimens prepared under nominally identical deposition conditions.

B. Experimental techniques

In this section, brief details are given of the experimental techniques employed to study the alloys. These are electron microprobe analysis, photoluminescence, photoconductivity, dc conductivity, optical and ir absorption, and transmission electron microscopy. A more detailed description of the electron microprobe, photoluminescence, and photoconductivity apparati can be found in Refs. 9, 31, and 32, respectively.

Electron microprobe analysis[9] was used to determine x, the atomic concentration of Ge relative to Si in the a-$Si_{1-x}Ge_x$:H alloys. The measurements were performed using a Cameca MBX unit with Tracor Northern automation on films grown on Cr-coated Corning 7059 glass. Probing several regions of each specimen indicated compositional nonuniformity of Si and Ge over areas 16×16 μm^2 of less than 1 at. %, the sensitivity of the probe.

Photoluminescence samples were deposited on 7059 glass substrates, which had been roughened so as to eliminate interference fringes. Steady-state photoluminescence spectra at 77 K were measured in reflection geometry using 2.41-eV Ar-ion laser excitation, a glass prism monochromator, and a thermoelectrically cooled PbS detector with lock-in detection. All spectra were corrected for system spectral response. The resolution of the measurement was approximately 0.02 eV.[31]

Room-temperature photoconductivity measurements[32] were carried out on films prepared on 7059 glass using a coplanar electrode configuration. Evaporated Cr contacts were found to have ohmic behavior both in the dark and under illumination over the range of the applied field used (50—500 V cm^{-1}). The photoconductivity was measured under our standard conditions, i.e., flux of 10^{15} photons $cm^{-2}s^{-1}$ at an energy of 1.96 eV. All values of photoconductivity in this paper are corrected for the penetration depth of the light in the samples as deduced from the optical-absorption spectra. The spectral dependence of the photoconductivity using the constant photocurrent method[33,34] was also investigated. These data were used to extend the optical-absorption spectra to lower energies.[32] The temperature dependence of the dark dc conductivity was also studied on similar structures over the range from about 294 K to about 475 K.

The optical transmission of films prepared on 7059 glass was measured using a Varian model no. 2390 double-beam spectrophotometer over the wavelength range 0.6 to 2.6 μm. Information was obtained on the optical-absorption edge, refractive index n, film thickness d, and the optical gap. We define the optical gap as E_{04},[35—38] the energy at which the optical-absorption coefficient, α, is equal to 10^4 cm^{-1}. From the transmission maxima, we obtain the position and order of the interference fringes in a nonabsorbing region of the spectra. To those we then fit a parabolic expression for n as a function of energy using an assumed approximate film thickness. The measured asymptotic transmission at 2 μm is then used to scale the deduced value of n and to provide a correct film thickness. These values were then used in the calculation of the optical-absorption coefficient, α, using standard optical formulae.[39]

The infrared-absorption spectra were recorded by a Perkin Elmer model no. 567 double-beam spectrometer. The spectra were obtained by placing a film (grown on roughened crystalline Si to eliminate interference fringes) in one beam and a matched piece of roughened crystalline Si in the reference beam. Spectra were taken in the frequency range between 200 and 4000 cm^{-1}. An estimate of the total hydrogen content, C_H, was obtained from the integrated absorption associated with the Si—H/Ge—H wag modes centered in the region 550—650 cm^{-1} using the expression

$$C_H = mA_w \ , \tag{1}$$

where C_H is in at. %, m is constant, and A_w (eV cm^{-1}) is the integrated absorption coefficient of the wag vibrations

calculated by a Gaussian fit. Respective values for m of 0.62, 0.37, and 0.39 at. %/eV cm^{-1} were taken for a-Si:H, a-Ge:H, and the alloys.[40–42]

Transmission electron microscopy was carried out on a variety of alloys prepared under different conditions using a Philips model no. EM 300 electron microscope. The films for this study were deposited directly on C-coated Ni microgrids. The C layer was about 100 Å thick, and the films about 500 Å, as deduced from the deposition rate and time.

III. VARIATION WITH T_s OF THE ELECTRICAL AND OPTICAL PROPERTIES OF a-$Si_{0.5}Ge_{0.5}$:H

It has been well established that the optical and electrical properties of glow discharge a-Si:H and a-Ge:H depend critically on the deposition temperature as a result of changes in the hydrogen content and the density of defects, which alter the size of the optical gap and the distribution of states in the band gap. Our first step in the study of a-$Si_{1-x}Ge_x$:H was to determine the optimum deposition temperature for films of roughly equal Si and Ge concentrations. We produced a series of samples holding all parameters constant except T_s, which was varied over the range 230 to 372 °C. The samples had good surface continuity, few pinholes, and excellent adhesion. The measurements described in Sec. II B were made on co-deposited samples. In Fig. 2, data are presented for the optical gap, E_{04}, the energy of the photoluminescence peak, E_{PL}, and the full width at half maximum of the peak, ΔE_{PL}, for the sample series. E_{04} and E_{PL} show the same linear decrease with increase of T_s. ΔE_{PL} is not a strong function of T_s. The hydrogen content, C_H, for these specimens was calculated from the integrated absorption of the infrared wag modes using Eq. (1). As shown in Fig. 3, C_H decreases monotonically from about 13 at. % at 230 °C to about 4 at. % at 372 °C.

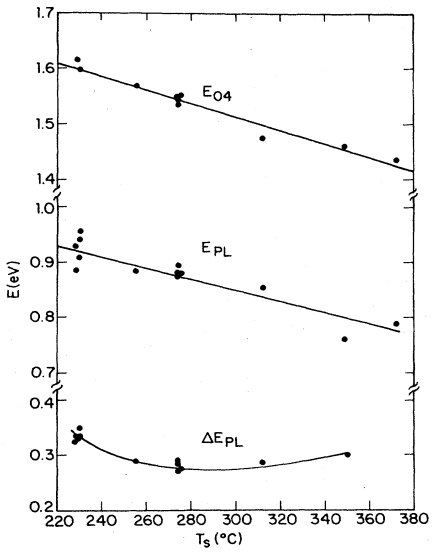

FIG. 2. Energy gap E_{04}, energy E_{PL}, and width ΔE_{PL} of the photoluminescence peak versus substrate temperature T_s for a-$Si_{0.5}Ge_{0.5}$:H.

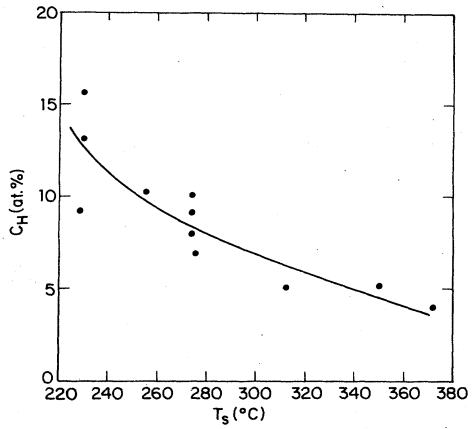

FIG. 3. Hydrogen content C_H versus substrate temperature T_s for a-$Si_{0.5}Ge_{0.5}$:H.

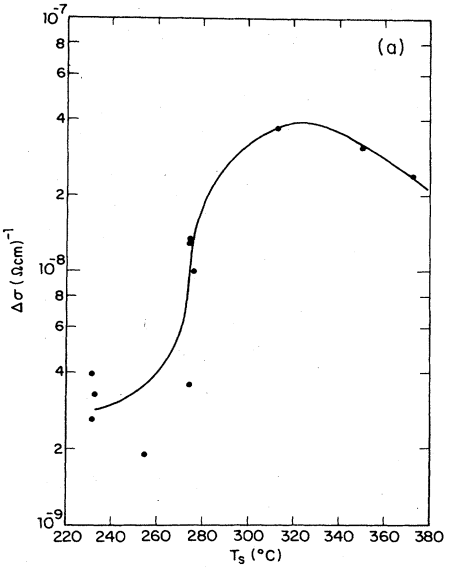

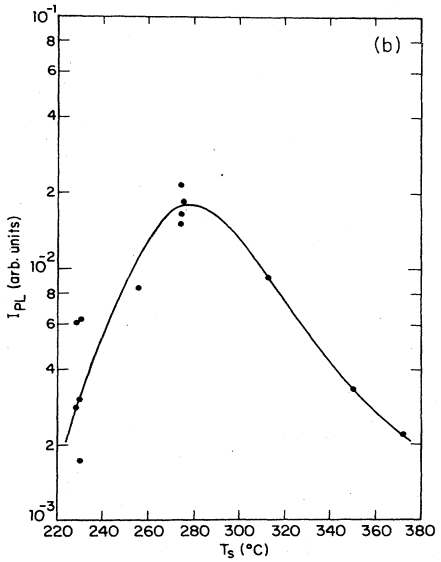

FIG. 4. (a) Photoconductivity $\Delta\sigma$ versus substrate temperature T_s for a-$Si_{0.5}Ge_{0.5}$:H. (b) Photoluminescence peak intensity I_{PL} versus substrate temperature T_s for a-$Si_{0.5}Ge_{0.5}$:H.

In Fig. 4, we show the photoconductivity, $\Delta\sigma$, and the photoluminescence peak intensity, I_{PL}, for the same series of samples. The magnitude of $\Delta\sigma$ is known to depend critically on the Fermi-level position. In the present series of specimens, the Fermi level is essentially independent of T_s, lying close to midgap, and we choose to use $\Delta\sigma$ as an indicator of the relative photoelectronic quality of the specimens. As shown in Fig. 4, the magnitudes of both $\Delta\sigma$ and I_{PL} initially rise by about an order of magnitude as a function of T_s and peak at around 300 °C. Above about 300 °C, I_{PL} decreases by an order of magnitude and $\Delta\sigma$ by a factor of 2. Because I_{PL} has been shown to correlate with the density of states near midgap in a-$Si_{1-x}Ge_x$:H (Ref. 20) and because $\Delta\sigma$ and I_{PL} are general indicators of the photoelectronic quality of the films, we use the deposition temperature of 300 °C, which provides close to the highest values of both these quantities in this film series, as the optimized substrate temperature for the a-$Si_{1-x}Ge_x$:H films prepared subsequent to this series.

We have also determined that the photoelectronic properties improved somewhat as the rf power was reduced below 3 W, but the improvement was not considered sufficient to offset the disadvantage of a decreased deposition rate (< 80 Å min^{-1}). Powers of 5 W, on the other hand, tended to produce samples with inferior physical properties. In consequence, a power level of 3 W was adopted for the study of alloys of different x.

IV. VARIATION WITH x OF THE ELECTRICAL AND OPTICAL PROPERTIES OF a-$Si_{1-x}Ge_x$:H

After optimization of the deposition parameters for a-$Si_{0.5}Ge_{0.5}$:H films, we kept these parameters fixed and varied the flow rate of the GeH_4 to produce samples of various compositions in the range of x from 0.14 to 0.74. We again measured the optical, electrical, and structural properties of the co-deposited samples.

In Fig. 5, absorption spectra are shown for a series of a-$Si_{1-x}Ge_x$:H alloys of different x prepared at 300 °C, together with data for an a-$Si_{0.98}Ge_{0.02}$:H alloy prepared at 230 °C, and an unalloyed a-Ge:H specimen prepared at 260 °C. The spectra of the alloys were extended to subband-gap energies using the constant photocurrent method.[33,34] The photoconductivity-derived part of the absorption spectrum was normalized to the part from direct optical transmission measurements in the range of overlap at higher photon energies in the band tails near an α of 10^3 cm^{-1}. In Fig. 5, the solid lines and the symbols denote the respective regions of the spectra deduced from optical transmission and from photoconductivity. The absorption spectrum of the a-$Si_{0.98}Ge_{0.02}$:H alloy is almost the same as that of a-Si:H. The spectra are observed to shift smoothly to lower energies and the subband-gap absorption to increase with Ge content. Also, the slope of the exponential edge, which can be accurately measured up to x of about 0.5, decreases with increasing Ge content by about 30%. We take this as an indication that alloying leads to an increase in the width of the valence-band tail. The oscillations observed in these spectra are caused by optical interference effects in the thin samples.

In Fig. 6, dark conductivity versus inverse temperature data are presented for some of the specimens from Fig. 5 and for representative samples of unalloyed a-Si:H and a-Ge:H. All specimens were heated under vacuum to about 210 °C before the measurements were performed, in order to ensure that any photoproduced defects (Staebler-Wronski effects[43]) were annealed out. All specimens exhibited activated transport and the conductivity, σ, is observed to increase with Ge content. For the alloys, σ is singly activated over almost 4 orders of magnitude. Figure 7 shows the variation with x of the transport activa-

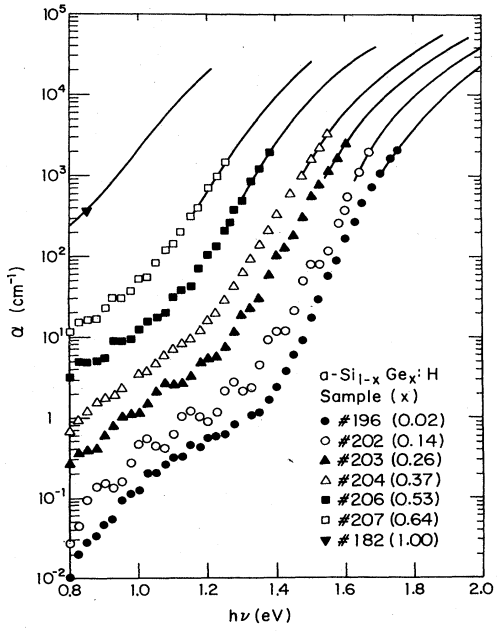

FIG. 5. Absorption coefficient α versus photon energy $h\nu$ for the a-$Si_{0.5}Ge_{0.5}$:H alloys indicated. The solid lines and symbols denote the respective regions of the spectra deduced from optical transmission and from photoconductivity.

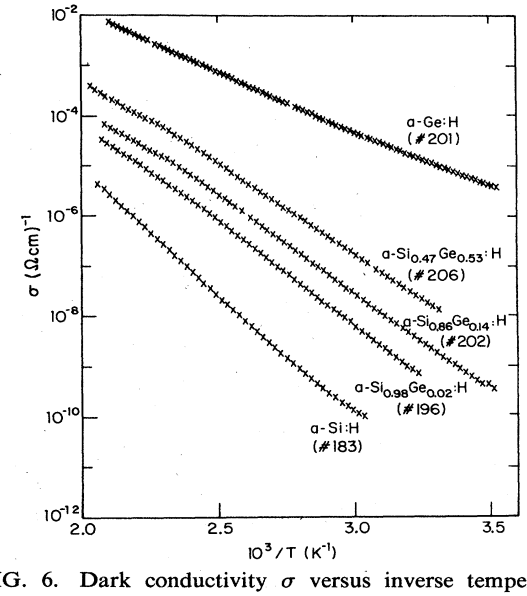

FIG. 6. Dark conductivity σ versus inverse temperature. The numbers in parentheses identify the samples.

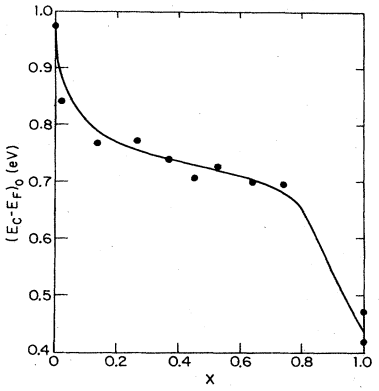

FIG. 7. Variation of the conductivity activation energy $(E_c - E_F)_0$ with x for the a-$Si_{1-x}Ge_x$:H alloys.

tion energy $(E_c - E_F)_0$, deduced by a fit of the conductivity data to the relation

$$\sigma = \sigma_0 \exp[-(E_c - E_F)_0 / kT] \,. \tag{2}$$

A downward kink in $\ln\sigma(1/T)$ is observed for temperatures greater than 150–160 °C (i.e., $10^3/T$ less than 2.31–2.36 K^{-1}) for alloys of composition $x = 0.14$ to 0.64 prepared at 300 °C and also for the a-$Si_{0.98}Ge_{0.02}$:H film prepared at 230 °C. The unalloyed specimens, particularly a-Ge:H, show signs of slight curvature in $\ln\sigma(1/T)$.

In Fig. 8 are presented the measured E_{04}, E_{PL}, and ΔE_{PL} for samples of the same series as reported in Fig. 5. There is a single photoluminescence band for all samples, except for the films with $x = 0.74$ and $x = 1$, where no photoluminescence was detected. Linear dependences on x are found:

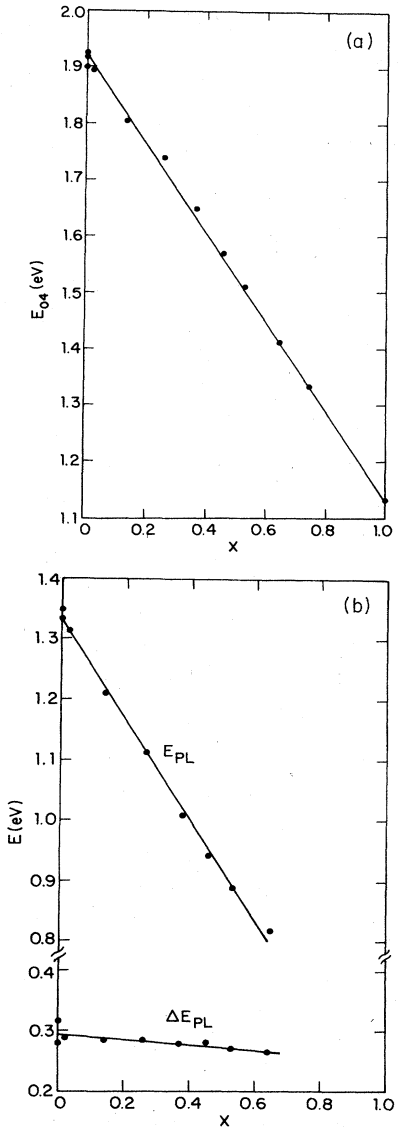

FIG. 8. (a) Energy gap E_{04} of a-$Si_{1-x}Ge_x$:H as a function of x. (b) Energy E_{PL} and width ΔE_{PL} of the photoluminescence peak of a-$Si_{1-x}Ge_x$:H as a function of x.

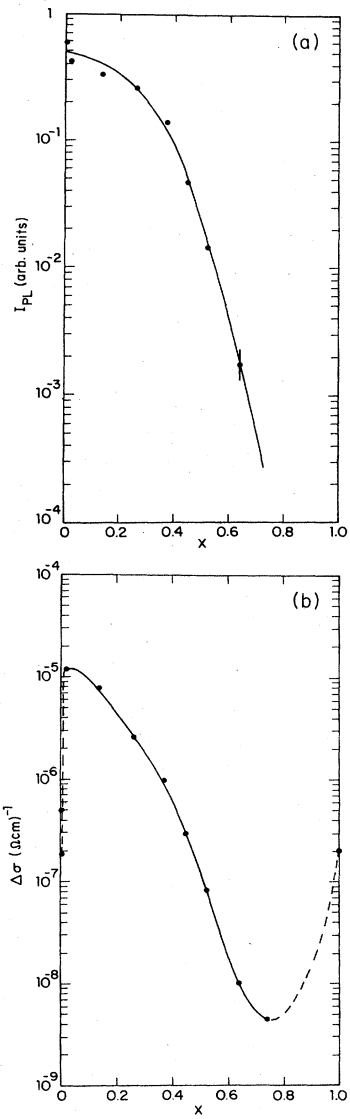

FIG. 9. (a) Variation of the photoluminescence peak intensity I_{PL} with x for a-$Si_{1-x}Ge_x$:H. (b) Variation of the photoconductivity $\Delta\sigma$ with x for a-$Si_{1-x}Ge_x$:H.

$$E_{04}=1.92-0.79x \text{ (eV)}, \quad (3)$$

$$E_{PL}=1.33-0.84x \text{ (eV)}, \quad (4)$$

$$\Delta E_{PL}=0.291-0.038x \text{ (eV)}. \quad (5)$$

It is essential to comment immediately that the influence of varying C_H on these relations is not clear. When the procedure to determine C_H from the integrated intensity of the wag modes in the infrared-absorption spectra is followed (see Sec. II B) C_H remains constant at about 8 at. % for x between 0 and 0.5. For $x>0.5$, C_H decreases and, in the unalloyed a-Ge:H samples, is only about 2 at. %. Given the sensitivity of E_{04} and E_{PL} to C_H in a-Si:H, one is surprised to find these parameters linearly dependent on x for $x>0.5$. Discussion of this will be taken up in Sec. VI B.

In Fig. 9 we show the photoluminescence peak intensity, I_{PL}, and the photoconductivity, $\Delta\sigma$, for these samples as a function of Ge content. I_{PL} initially falls off gradually with Ge content up to $x\sim 0.3$ then decreases rapidly by almost 3 orders of magnitude. $\Delta\sigma$ exhibits a similar behavior with x. However, beyond $x=0.74$, $\Delta\sigma$ is observed to increase. It is interesting that alloying a-Si:H with as little as 2 at. % Ge leads to a large improvement in $\Delta\sigma$. In considering an explanation of these results we must bear in mind that between $x=0$ and $x=0.02$ and between $x=0.74$ and $x=1.0$ the Fermi level (as deduced from the activation energy for conductivity) approaches the conduction-band edge.

V. STRUCTURAL PROPERTIES OF THE a-$Si_{1-x}Ge_x$:H ALLOYS

In this section, results are presented on a structural examination of the a-$Si_{1-x}Ge_x$:H alloys using infrared spectroscopy and transmission electron microscopy. In particular, results are presented on the structural properties of a-$Si_{0.5}Ge_{0.5}$:H as a function of T_s and also a-$Si_{1-x}Ge_x$:H prepared at 300 °C as a function of x.

Figure 10 shows the infrared-absorption spectra of a-$Si_{0.5}Ge_{0.5}$:H grown at (a) 230 °C, (b) 275 °C, and (c) 312 °C. The three alloys are of similar thickness. The main absorption features are labeled in (a). The modes at 2000 and 2090 cm^{-1} are stretch modes associated with Si-H entities. The corresponding stretch modes for Ge-H are at 1875 and 1975 cm^{-1}.[44–51] The features near 845 and 885 cm^{-1} are bending modes related to $(SiH_2)_n$ complexes.[52] The wagging modes from which C_H was calculated are centered at about 630 cm^{-1}. At the lowest T_s of 230 °C, the Si—H bending modes are at their largest. The Si—H stretch mode is mainly centered at 2090 cm^{-1}. Increasing T_s results in an increase in the intensity of 2000-cm^{-1} absorption relative to the 2090-cm^{-1} mode. At T_s of 312 °C, the 2000-cm^{-1} mode is now dominant over the 2090-cm^{-1} modes and the Si—H bending modes are much less prominent. The infrared-absorption spectra of the a-$Si_{1-x}Ge_x$:H alloys prepared at 300 °C have also been studied. The addition of 14 at. % Ge to a-Si:H does not lead to any appreciable changes in the absorption spectra, i.e, the Si—H stretch mode at 2000 cm^{-1} is dominant and the Si—H bending modes are very small. With increasing Ge

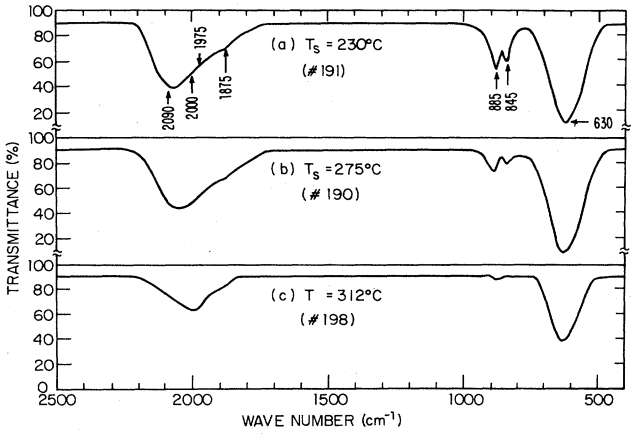

FIG. 10. Infrared spectra of a-$Si_{0.5}Ge_{0.5}$:H prepared at T_s = (a)230 °C, (b) 275 °C, and (c) 312 °C. The main absorption features are labeled in (a). The numbers in parentheses identify the samples.

content, the Ge—H stretch modes increase, as does the 2090-cm^{-1} mode, however, the 2000-cm^{-1} mode remains dominant. The Si—H bending modes remain very small.

The spectra of the a-$Si_{1-x}Ge_x$:H alloys are recorded immediately upon removal from the UHV deposition chamber. The spectra of several different types of specimens have been monitored closely as a function of time after the initial measurement. It is found that when the 2090-cm^{-1} mode is dominant over the 2000-cm^{-1} mode, e.g., a-$Si_{0.5}Ge_{0.5}$:H prepared at $T_s=230$ °C, films show signs of oxygen incorporation from the atmosphere. Figure 11 shows the changes in the measured absorption spectra with time of an a-$Si_{0.5}Ge_{0.5}$:H specimen grown at 230 °C. After a few days a broad absorption band between 800 and 1200 cm^{-1} becomes evident and then is observed to rapidly increase in magnitude with time. This band has been attributed to oxygen incorporation.[53] Superimposed on this band are modes at 980 and 1050 cm^{-1} which are associated with Si-O entities. On some samples, a distinct distortion in the Si—H bending modes is observed. This may be due to the presence of a Ge—O vibrational mode at 860 cm^{-1}.[54] (The unalloyed a-Ge:H films prepared for

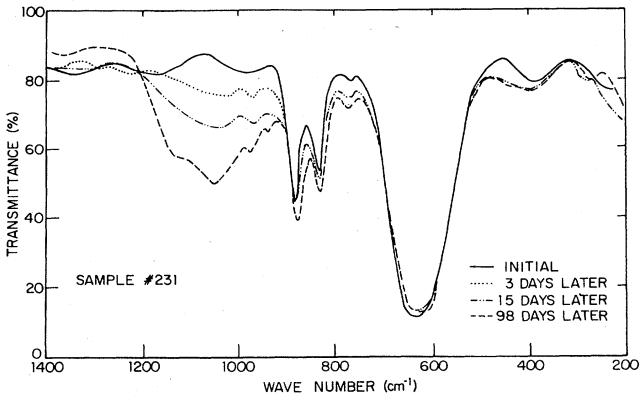

FIG. 11. Changes in the infrared spectrum with time of an a-$Si_{0.5}Ge_{0.5}$:H sample prepared at 230 °C.

this work showed strong evidence of a vibrational mode at 860 cm^{-1}. The intensity of this absorption is observed to grow rapidly with time.) An estimate of the oxygen content in the a-$Si_{0.5}Ge_{0.5}$:H alloy was calculated from the expression,

$$C_O = mA_O , \quad (6)$$

where C_O is the atomic percentage of oxygen, m is a constant ($=0.156$ at. %/eV cm^{-1}),[55] and A_O is the measured integrated absorption coefficient of the Si—O bond centered at 1050 cm^{-1}. Figure 12 shows the estimated oxygen content of the a-$Si_{0.5}Ge_{0.5}$:H sample from Fig. 11 as a function of time. The oxygen content is of the order of a few percent. Also included in the figure for comparison are results for an a-$Si_{0.5}Ge_{0.5}$:H specimen prepared similarly but covered with about 1000 Å of a-Si:H. The a-Si:H layer reduces the rate of oxygen uptake, demonstrating the atmospheric origin of the oxygen.

Figure 13 shows transmission electron microscopy (TEM) photographs of a-$Si_{0.5}Ge_{0.5}$:H prepared at 230 °C and 300 °C. Both specimens exhibit microstructure in the form of noncoalescing regions of high electron density in a honeycomb network of lower density material. These regions are of the order of 100—500 Å in size. On average, the dimensions of the regions in the specimen prepared at 300 °C are much smaller than for the films deposited at 230 °C. No clearly discernible microstructure

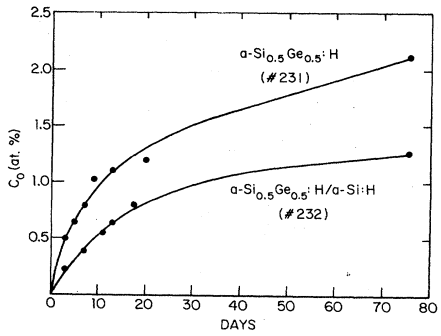

FIG. 12. Estimated oxygen content C_O as a function of time for the a-$Si_{0.5}Ge_{0.5}$:H sample from Fig. 11. For comparison, results are shown for a similarly prepared alloy capped with a-Si:H. The numbers in parentheses identify the samples.

of this nature was observed in our unalloyed a-Si:H films. However, the unalloyed a-Ge:H samples showed microstructure on a scale of about 200 Å.

VI. DISCUSSION

A. Variation with T_s of the electrical and optical properties of a-$Si_{0.5}Ge_{0.5}$H

The effect of an increase of preparation substrate temperature, T_s, on the properties of *unhydrogenated* a-

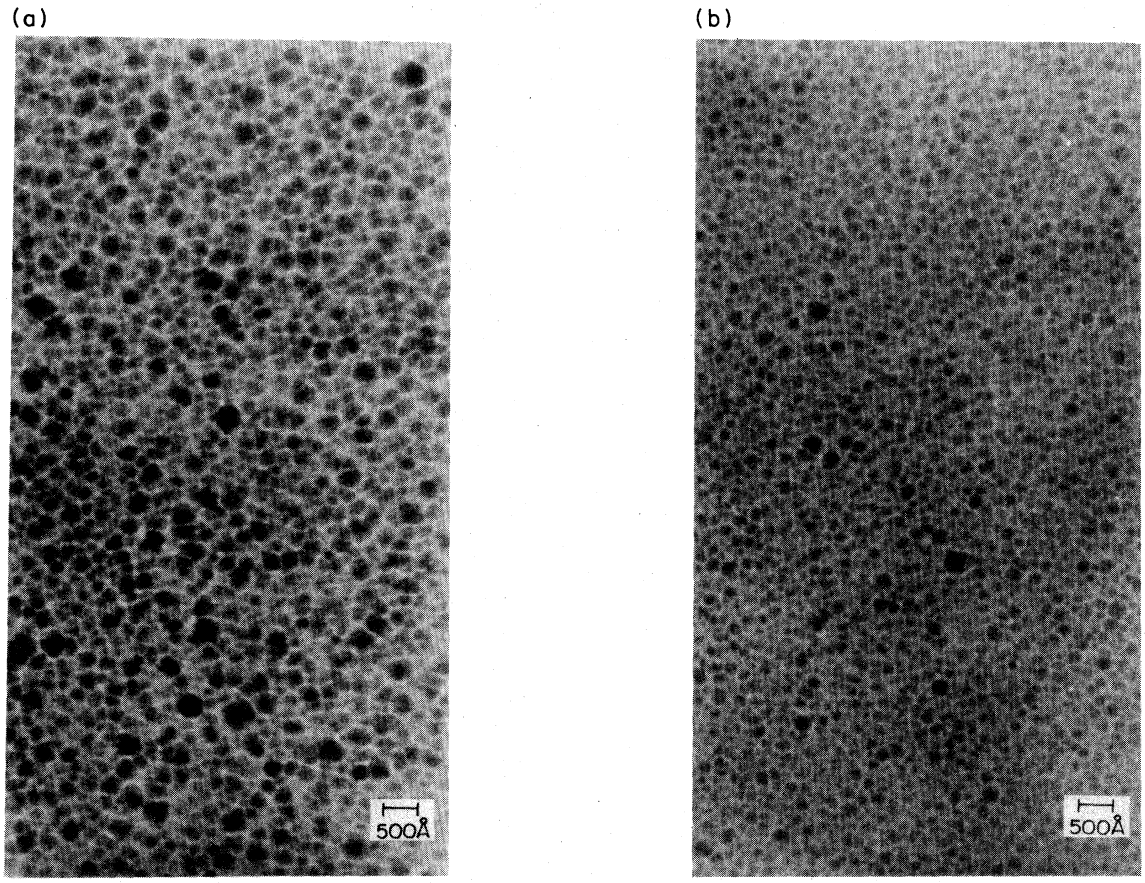

FIG. 13. Bright field TEM images of a-$Si_{0.5}Ge_{0.5}$:H prepared at (a) 230 °C and (b) 300 °C.

Ge,[5,56–58] *a*-Si,[5] and *a*-$Si_{1-x}Ge_x$,[5] has already been studied. Among the results universally reported are a sharpening and a shift to higher photon energies of the optical-absorption edge, and an increase in the photoconductivity. These and other results are consistent with a decrease in the density of states (DOS) near the edges of the valence and conduction bands, in the band tails, and in the band gap, and these in turn are consistent with the healing of the disordered network, both to decrease the topological disorder of the completely coordinated structure and to reduce the number of defects such as dangling bonds. It seems reasonable to expect the same effects for increases in T_s for *hydrogenated* material.

The effect of an increase in T_s for *hydrogenated* material must, however, also take account of any changes in C_H with T_s. The variation of C_H with T_s for our samples of *a*-$Si_{0.5}Ge_{0.5}$:H is shown in Fig. 3. While this variation may be expected to depend in its detail on the method of preparation, the decrease in C_H with increase in T_s is qualitatively consistent with published data on *a*-Si:H.[59] It is also consistent with studies of the evolution of hydrogen when *a*-Si:H is annealed.[60]

The effect of *increased* C_H alone on the topological disorder, the defect density, and the electronic band structure is essentially equivalent to that of increased T_s for the unhydrogenated material: The hydrogen compensates dangling bonds, thus reducing the midgap state density; the hydrogen also forms a Si—H alloy, with reduced densities of states at the former valence- and conduction-band edges; and, by reducing the average coordination number, it facilitates a structure with smaller topological disorder. The overall results for changes with T_s of the properties of the present hydrogenated alloys, taking into account both the effects of changing C_H and the explicit temperature effect, should be interpreted within this general framework.

We discuss first the linear decreases, at the same rate, of E_{04} and E_{PL} between 230 and 372 °C shown in Fig. 2. Apparently, for this range of T_s, the effect of a decrease in C_H with T_s is more important than the effect of network healing. This result is qualitatively consistent with earlier work that may be taken to estimate the two effects of T_s separately. (1) The explicit effect of T_s may be estimated from the change in optical gap of *unhydrogenated* *a*-Si, *a*-Ge, and *a*-$Si_{1-x}Ge_x$. Thus, Connell *et al.*[58] found a change of 0.2 eV for a T_s increase from 25 °C to 350 °C for *a*-Ge, while Paul *et al.*[5] found an increase of at most 0.08 eV for a T_s increase from 200 °C to 550 °C for *a*-Si, and of 0.1 eV for a T_s increase from 100 °C to 350 °C for *a*-$Si_{0.45}Ge_{0.55}$. (2) The effect of decrease in C_H with increase in T_s may be estimated from the change in optical gap of *a*-Si:H when C_H is changed at fixed T_s, as happens when the partial pressure of H_2 is changed in the sputtering method of preparation. Such studies by ourselves suggest[61] a decrease in gap of about 0.5 eV when C_H is decreased from 15 at. % to 2 at. %, while Morel and Moustakas[62] find a decrease of about 0.25 eV for a similar decrease in C_H.

Combining these (admittedly) disparate sources of data suggests that an increase in T_s from 230 °C to 372 °C would lead to an increase in gap of about 0.06 eV due to the explicit T_s effect, and a decrease of about 0.17 to 0.35 eV due to the C_H decrease. Thus, the actual experimental finding is rationalized.

Next we consider the changes with T_s of the electron photoconductivity, $\Delta\sigma$, and the photoluminescence peak intensity, I_{PL}, for *a*-$Si_{0.5}Ge_{0.5}$:H shown in Fig. 4. The existence of an optimum T_s for the photoconductivity of rf glow discharge *a*-$Si_{1-x}Ge_x$:H alloys has also been reported by Nakamura *et al.*[63] (200—250 °C) and by Bullot *et al.*[11] (280 °C). We expect that the optimum T_s will depend on the method of preparation, the deposition system, and the Ge content. Taking into account also that the deposition temperature T_s is measured in different ways, the experimental observations in the literature may be taken as self-consistent.

The magnitude of $\Delta\sigma$ depends on the electron trapping lifetime which is determined by the DOS distribution above the Fermi level and so by the energetic position of the Fermi level below the conduction band. However, for the *a*-$Si_{0.5}Ge_{0.5}$:H films investigated, the transport activation energy decreases by only 0.14 eV as T_s is varied from 230 °C to 372 °C. This small change suggests that the *initial* rapid increase of $\Delta\sigma$ with T_s is attributable to a decrease in the DOS just above E_F. The initial rapid increase in I_{PL} is similarly consistent with a decrease in gap DOS; this correlation has been recently explicitly demonstrated for *a*-$Si_{0.7}Ge_{0.3}$:H (Ref. 20) and *a*-Si:H (Ref. 31) through a comparison of PL magnitudes and the midgap state densities. Much recent work demonstrating that $\Delta\sigma$ and I_{PL} increase with decreasing density of dangling bonds is suggestive of a decrease in such density in the present instance, but we have no explicit experimental proof identifying this defect as the cause.

The *initial* increases in $\Delta\sigma$ and I_{PL} are consistent with the explicit effect of temperature (T_s) rise in reducing the midgap DOS, and they imply that this effect overrides the effect of an increase in midgap DOS consequent on a decrease in C_H. We recall that the net result on E_{04} and E_{PL} of the two effects of an increase in T_s favored the dominance of the C_H decrease in the temperature range of 230 °C to 300 °C. These results may be reconciled if we infer that the explicit T_s effect is less important than the decrease in C_H in affecting the DOS near the valence- and conduction-band edges, but more important in affecting the midgap DOS.

For $T_s \geq 300$ °C, E_{04}, E_{PL}, $\Delta\sigma$, and I_{PL} all decrease. This is consistent with the overriding effect of decreasing C_H in increasing the DOS throughout the entire energy gap. The monotonic decrease of E_{04} and E_{PL} over the full range of T_s, and the maxima in $\Delta\sigma$ and I_{PL} near 300 °C, are therefore assigned to a change in the relative effects of decrease in C_H and increase in network and defect healing. We may proceed further, in more speculative fashion. Early work by Paul *et al.*[56–58] and Paesler *et al.*[64] on unhydrogenated *a*-Ge showed that a sharp change in a variety of properties (density, refractive index, porosity, internal stress, and free spin density) occurred for T_s near 300 °C, and this was attributed to a rapid change in the structure of the films near this T_s. This rapid change was related to the probability that an adatom configuration on the growth surface would transform to a

lower energy adatom configuration during the time for deposition of a monolayer. We may therefore speculate that up to a T_s of about 300 °C a major effect is the removal of defects associated with Ge, which more than compensates for any loss in hydrogen content, but that, after this process is completed, the effect of hydrogen content reduction dominates the outcome.

B. Variation with x of the electrical and optical properties of a-$Si_{1-x}Ge_x$:H

The observed changes in optical and transport properties as x is varied are consistent with our earlier reports[8,9] on this subject and with publications by other workers.[10] In this section we shall try to advance the interpretation, using our extensive data on co-deposited samples, and appealing to new knowledge about the energies of defect levels. We recall from Secs. IV and V the principal findings. (1) As x is increased, the energy gap, E_{04}, and the photon energy, E_{PL}, corresponding to the peak of the photoluminescence spectrum decrease linearly and almost exactly at the same rate. (2) As x is increased from 0 to 0.64 the magnitude of the PL intensity, I_{PL}, decreases by a factor of about 250. Beyond $x=0.64$, we are unable to detect PL. (3) As x is increased from 0 to 0.74, the magnitude of the photoconductivity response for $h\nu=1.96$ eV decreases rapidly. For pure a-Ge:H, it is nearly 2 orders of magnitude larger. (4) As x is first increased to about 0.37, the magnitude of the subband-gap absorption [for brevity referred to as $\alpha(1.2)$] increases, until the effect is obscured at small values of the energy gap. (5) As x is increased, the infrared-vibrational-absorption spectra change in a way suggesting structural alterations. (6) For high Ge content and low T_s, there is evidence of oxygen contamination and in-diffusion with time. (7) Electron microscopy studies suggest the existence of heterostructure in the a-$Si_{0.5}Ge_{0.5}$:H films. We recall also (1) a demonstrated correlation between decreased I_{PL} and increased midgap DOS (derived from SCLC measurements) in a-$Si_{0.7}Ge_{0.3}$:H alloys,[20] which suggests that the midgap states (dangling bonds?) act as nonradiative recombination channels, (2) a demonstrated correlation for a-Si:H between the magnitude of midgap DOS (derived from admittance measurements) and the subband-gap absorption $\alpha(1.2)$,[65] (3) preliminary SCLC measurements on the alloys which suggest an increase in midgap DOS with increasing Ge content.[66] For unalloyed a-Si:H prepared at 230 °C the DOS is about 3×10^{15} $cm^{-3}eV^{-1}$, for $x=0.02$ the DOS is about a factor of 4 higher, while for $x=0.5$ ($T_s=300$ °C) the DOS is about 10^{17} $cm^{-3}eV^{-1}$. We recall also (4) that increases in the DOS in the gap on Ge alloying have been deduced by Huang *et al.*[67] from SCLC measurements and by Senemaud *et al.*[68] from a combination of photoemission and subband-gap absorption.

The linear decrease of energy gap (in whatever manner it is estimated) with x has been the conclusion of most published work.[69] The parallel decrease of E_{PL} with x is consistent with the interpretation of the radiative transition as conduction-band tail to valence-band tail. The linear decrease of ΔE_{PL} with x, taken together with the (small) increase in width of the valence-band tail inferred from the decrease in slope of the exponential part of the absorption edge, suggests a (slight) sharpening of the tail to the conduction-band edge.

These simple conclusions are vitiated to some extent by doubts concerning the possible influence of C_H variation with x. Some of the work reported in the literature did not consider, or at least did not discuss, the determination of C_H.[8,9] In the present work (see Sec. IV) C_H remains constant for $0\le x\le0.5$, but decreases for $x>0.5$. We have no fully satisfactory explanation for the continued (rather good) linear dependence of E_{04}, E_{PL}, and ΔE_{PL} on x for $x>0.5$, but the following observations may be pertinent. First, the procedure of obtaining C_H from infrared-absorption calibrated by nuclear reaction results may be inappropriate if the latter experiments measure all H, strongly and weakly bonded, while the former measures only the strongly bonded fraction. Second, there is good evidence that the films are heterogeneous, which may imply a nonuniform distribution of H over those regions determining the optical-absorption properties and the regions which do not. Third, there appears to be a difference between the gap increase caused by hydrogenation of a-Ge and a-Si. Thus, films of a-Ge prepared at high temperatures have values of E_{04} of about 1.1 eV.[70] Addition of $\sim$8 at. % H was estimated to increase E_{04} to 1.2 eV by Connell and Pawlik[71] and addition of $\sim$10 at. % H to increase E_{04} to 1.2 eV by Rudder *et al.*[72] On the other hand, unhydrogenated a-Si prepared at 200 °C has an E_{04} of about 1.4 eV, and hydrogenation to $\sim$10 at. % increases E_{04} to 1.9 eV.[61]

Clearly, however, more work is needed to clarify the dependences of the energy gap on x and C_H described here. We note in passing that it is essential that the value of x be determined from examination of the films by electron microprobe (as was done here) or similar measure, and not by the ratio of GeH_4 to SiH_4 in the plasma.[73]

We next discuss the important question of the energy of the defect states. In principle, there can be a variety of defects in the band-gap dangling bonds, reconstructed bonds longer in spatial extent and weaker in bond strength than the normal Si—Si covalent bonds, bipolaron reconstructions, and the like.[74] Much recent work has shown that, to a high degree of probability, the dominant defect giving states in the upper half of the gap of a-Si:H is the dangling bond, either neutral D^0 or doubly occupied D^-. We feel that it is very likely that the lower half of the gap of a-Si:H contains states attributable to the other types of defects, not yet fully explored. It is not clear whether this neat division of roles for dangling bonds vis-à-vis with the rest pertains in the alloys and in a-Ge:H, but we shall tentatively assume this is so, and concentrate our attention on the dangling-bond states. Although the assembly of results just described appears to suggest an increase in dangling-bond density with x, it behooves us to consider first effects that may ensue from changes in the gap density of states (GDOS) *distribution relative to the Fermi level,* independent of changes in the total integrated GDOS. We suppose that the "absolute" energy (with respect to, say, the vacuum level) of a dangling-bond state D^0 or D^- on either a Si or a Ge atom remains essentially constant as x is changed. The fact that the g values for the singly-

occupied dangling bonds do not change with x supports this contention.[21] We suppose also that the widths of the D^0 and D^- bands do not change with x, since the topologies of a-Si:H and a-Ge:H are similar, and we shall assign to them a FWHM of 0.2 eV. Further, we suppose that the correlation energies $[E(D^-)-E(D^0)]$ remain unchanged at 0.35 eV for Si (Ref. 75) and 0.1 eV for Ge (Ref. 76) as x is varied. Also, we place the D^0 band at 1.0 eV below E_c in Si (Refs. 77–81) and at 0.5 eV below E_c in Ge.[82]

Finally, it is necessary to include the variation with x of the absolute energies of E_c and E_v. We have found it to be quite difficult to estimate these accurately by considering the results of photoemission from valence-band and core levels. The problem is the same as that faced by workers on valence- and conduction-band discontinuities in semiconductor heterostructures. After following an iterative process of postulating the variations of $E_c(x)$ and $E_v(x)$ which fitted the observed $E_{04}(x)$, and considering the inferences for the photoconductivity, we concluded that it was most reasonable to suppose that E_v increased, and E_c decreased, at the same rate with x.[83]

Figure 14 thus shows the variation of E_v, E_c, and the $E(D^0)$ and $E(D^-)$ for Ge and Si dangling bonds as x is varied from 0 to 1. It should be emphasized that this diagram is a schematic of the distribution of states in these materials, showing only the band-edge energies, the centers of the dangling-bond bands, and the Fermi energy as a function of x. We have assumed E_c-E_v to be 1.8 eV for a-Si:H and 1.0 eV for a-Ge:H; there is a certain arbitrariness to this choice (see Ref. 35), but it fits with our conclusion from previous research that the band gap is probably a little smaller than E_{04} (1.9 eV for our a-Si:H and 1.1 eV for our a-Ge:H).

We have also sketched in Fig. 14 the variation of E_F, which is assumed to be given by the value of the transport activation energy from Fig. 7. The important point, which may then be noted from Fig. 14, is that there is a change in the relative filling of the dangling-bond states with x. Thus, as E_F approaches closer to the valence-band [because of the small change in $(E_c-E_F)_0$], more dangling-bond states become more positively charged.

In Fig. 15 we have schematized the band structure for

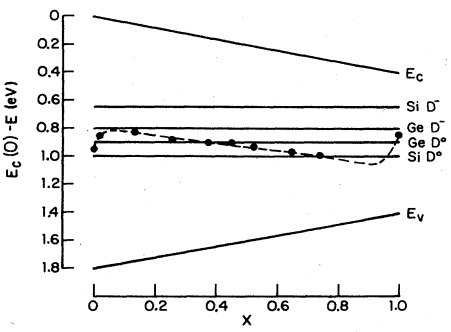

FIG. 14. The variation of E_v, E_c, and the $E(D^0)$ and $E(D^-)$ for Ge and Si dangling bonds as x is varied from 0 to 1. The dashed line and points indicate the variation of E_F with x deduced from the conductivity activation energy $(E_c-E_F)_0$.

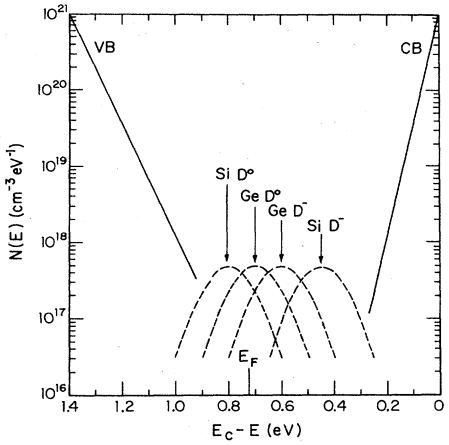

FIG. 15. Schematic band structure for a-$Si_{0.5}Ge_{0.5}$:H showing the location of the Si and Ge D^0 and D^- dangling-bond centers with respect to the conduction and valence bands (CB and VB).

the a-$Si_{0.5}Ge_{0.5}$:H alloy, assuming the same dangling-bond density of 10^{17} cm^{-3} for Si and Ge. We emphasize two points. First, several tentative assumptions have entered into the construction of Figs. 14 and 15, but we believe that only modifications of these diagrams will be required, as better estimates of parameter variation with x are established, and not abandonment of the overall approach. Second, there is good reason to believe that increases in defect density and changes in microstructure with x must also be considered in developing an overall description. We consider this next.

Increases in the defect density with x are suggested not only by the decreases in $\Delta\sigma$ and I_{PL}, but also by the subband-gap absorption and direct SCLC measurement. However, it must be noted that subband-gap absorption has two origins, one a transition from the valence band into empty states above E_F and the other a transition from below E_F into the conduction band. These two optical transitions do not necessarily have the same matrix element. Deductions about the DOS from spectra of $\alpha(h\nu)$ [and also, of course, deductions of $\alpha(h\nu)$ from $\Delta\sigma(h\nu)$] must be considered in the framework of Figs. 14 and 15. Similar remarks apply to the DOS determined by SCLC or indeed any other such measurements: while the DOS at a specified energy may be determined, its meaning in terms of defect density requires a consideration of the changes with x in placement of E_v, E_c, and the defect energy levels.

We consider finally the implications for the photoelectronic properties of Figs. 14 and 15. The variations with x of E_{04}, E_{PL}, and ΔE_{PL} have, of course, been incorporated into the figures. The most important point is that, as an increasing fraction of a constant density of dangling-bond states become more positively charged with increase of x, the magnitude of the photoluminescence and the photoconductivity will decrease. An increase of dangling-bond density with x will simply increase this effect. The magnitude of the subband-gap absorption will

change, even for constant density of dangling bonds, if the matrix elements for transitions from valence-band states to empty dangling-bond states and from filled dangling-bond states to conduction-band states are different. Again, an increase in density of dangling bonds will emphasize this effect. That such an increase in defects is very plausible is strongly suggested by the structural studies based on infrared spectroscopy and transmission electron microscopy. We discuss these in more detail next.

C. Variation with T_s and x of the positive evidence for structural heterogeneity

In this section we shall argue that lower T_s and higher x lead to greater heterogeneity in the films, that is, more specifically, to a greater difference in physical properties between growth islands and the tissue connecting them.[84]

1. *Infrared vibrational absorption*

Wagner and Beyer[51] have shown for a-Si:H that the occurrence of aSi—H stretch mode near 2100 cm^{-1} correlates with structural inhomogeneity.[85] Our results are consistent with their findings. The infrared-absorption spectra displayed in Fig. 10 for a-$Si_{0.5}Ge_{0.5}$:H indicate the appearance, increase in intensity, and eventual dominance of the 2090-cm^{-1} mode over the 2000-cm^{-1} mode as T_s is decreased from 312 °C to 230 °C. Moreover, films grown at $T_s < 300$ °C show signs of continuous oxygen incorporation from the atmosphere (Fig. 12). Presumably the oxygen diffuses into the film more readily via low atomic density tissue and some of it chemically bonds to the Si. Knights *et al.*[86] and Ross and Messier[87] have previously reported oxygen incorporation in a-Si:H when the 2090-cm^{-1} mode and bending modes between 800 and 900 cm^{-1} are present.

A strong 2090-cm^{-1} mode and much oxygen indiffusion become more likely as x is increased. Thus, unalloyed a-Si:H and a-$Si_{0.98}Ge_{0.02}$:H prepared at 230 °C show no sign of either, while for unalloyed a-Ge:H the 1975-cm^{-1} high-frequency component of the Ge-H stretch doublet is usually present (this corresponds to the 2090-cm^{-1} Si—H stretch mode) and oxygen incorporation occurs.

2. *Transmission electron microscopy*

Direct evidence of structural inhomogeneity in a-$Si_{0.5}Ge_{0.5}$:H is seen in the TEM micrographs shown as Fig. 13. The high-density regions are of the order of 100—500 Å across. On average, the dimensions of these regions in the specimens grown at 300 °C are much smaller than in films prepared at 230 °C, implying that the higher T_s films are more structurally homogeneous. The a-Ge:H also showed discernible microstructure on a scale of 200 Å but, by contrast, no clearly discernible structure was found in our unalloyed a-Si:H. We emphasize that this does not rule out the possibility of its presence and, in fact, microstructure has been observed elsewhere in high quality a-Si:H.[88] We are of the view that it is always present as a consequence of the mechanism of film growth under our preparation conditions. The question is one of the discernibility in a TEM which has to do with differences in atom density between island and tissue.

3. *High-temperature kinks in $\ln\sigma$ versus $1/T$*

Decreases in the slope of $\ln\sigma$ versus $1/T$ plots at high temperature ($10^3/T \lesssim 2.4$ K^{-1}) have been found by many workers,[89] and further examples may be seen in Fig. 6. Anderson and Paul[90] have proposed to explain these so-called kinks on the basis of a model[91] of a heterogeneous film structure consisting of high atom density islands interconnected by low atom density tissue. In the islands, most of the dangling bonds are compensated by hydrogen, probably in the monohydride Si-H configuration. In the tissue, there is a larger density of defects and a greater variety of Si—H bonding entities. Island and tissue therefore have different structure, chemistry, and transport properties. In a heterogeneous film, it is supposed that neither phase is likely to form a continuous (electrical) channel between electrical contacts. In their model, the measured conductivity is determined by the island material below the "kink", and by the tissue material at high temperatures. The kink occurs because island and tissue possess different σ *versus* $1/T$ characteristics.

A different explanation for these kinks has been put forward by Overhof and Beyer.[92] In their model, the kink is produced by a rapid change of the dependence of the Fermi level on temperature near the kink temperature. This rapid change is linked to the occurrence of fluctuations in the potential. It is to be noted that the presence of heterostructure in the form of islands and tissue is a very likely cause of potential fluctuations on the scale desired, so that both explanations for the kinks in $\ln\sigma$ correlate them with increasing heterogeneity.

The present results on a-$Si_{1-x}Ge_x$:H are only partly supportive of the suggested connection between heterogeneity and kinks in $\ln\sigma$ versus $1/T$. Thus, in Fig. 6, unalloyed a-Si:H does not show a kink, while the Si—Ge alloys do, in agreement with our hypothesis that increasing x induces heterostructure. On the other hand, the a-Ge:H sample of that figure does not show a kink. It is also to be noted that a sample of a-$Si_{0.98}Ge_{0.02}$:H prepared at $T_s = 230$ °C shows a kink, yet its infrared spectrum is very similar to that of unalloyed a-Si:H viz. a dominant 2000-cm^{-1} mode and no bending modes near 800—900 cm^{-1}. Further, a sample of a-$Si_{0.5}Ge_{0.5}$:H prepared at 230 °C does not show a kink, yet has a dominant absorption at 2090 cm^{-1} and strong bending modes. We are forced to conclude from this confusion of indicators that this transport anomaly is a poor guide concerning structure for the present set of films.

4. *Evolution of hydrogen*

Although not reported in detail in this paper, it is pertinent to draw attention to our earlier work[17] on the thermal evolution of hydrogen from films of a-$Si_{1-x}Ge_x$:H of different x produced by dc glow discharge at different T_s. The general conclusion of that work firmly supported the present interpretation viz. that low

T_s and increased x produced films which showed evolution of H at low temperatures (order of 200 °C), which implied the existence of easy exit pathways for H_2 molecules—presumably through low-density tissue.

VII. CONCLUSIONS

The principal conclusions from this work are the following.

(1) Increased substrate temperature T_s affects the properties of a-$Si_{0.5}Ge_{0.5}$:H both through increased network healing and decreased H incorporation. The observed results include a linear decrease of the optical energy gap and the peak energy of photoluminescent emission over the full range of T_s and a maximum in the magnitude of photoluminescence intensity and photoconductivity response for T_s near 300 °C.

(a) For T_s increasing below 300 °C, the network healing effect reduces the state density in the energy gap (GDOS), while the decrease in H content increases it. In this temperature range, the former effect is more important in causing a net decrease in GDOS near midgap and the latter effect more important in producing a net increase in GDOS near the valence- and conduction-band edges.

(b) For T_s increasing beyond 300 °C the increase in DOS throughout the band gap caused by decreasing the H content is the overriding effect.

(c) The maximum in photoconductivity and photoluminescence near $T_s = 300$ °C, supposedly caused by a change in the relative importance of network healing and H removal in affecting the midgap DOS, may be connected with a critical T_s for the elimination of a fundamental defect primarily associated with the Ge.

(2) Increased substrate temperature favors the production of films which have less visible heterostructure, as inferred from studies of infrared vibrational absorption, transmission electron microscopy, and hydrogen evolution. Also, the films produced at high T_s (≈ 300 °C) show less evidence of oxygen contamination and in-diffusion with time.

(3) For $T_s = 300$ °C, increased Ge content x produces the following changes: (a) The optical energy gap and the peak energy of photoluminescent emission decrease linearly at the same rate; (b) the magnitude of the intensity of photoluminescence decreases by 3 orders of magnitude (by $x = 0.74$) and falls below our detection limit; (c) the magnitude of the photoconductivity decreases rapidly but recovers near $x = 1$; (d) the magnitude of the subband-gap absorption increases; (e) the infrared-vibrational-absorption spectra change in a way suggesting alterations of structure.

(4) A band structure may be constructed for a-$Si_{1-x}Ge_x$:H alloys based on the following observations and assumptions: (a) The energy gap decreases linearly with x from 1.8 eV to 1.0 eV; (b) the principal defect states, at least in the upper half of the band gap, are caused by dangling bonds on the Ge and Si atoms. The energies of the singly-occupied (D^0) and doubly-occupied (D^-) dangling-bond states may be taken, with some uncertainty, from current work on spin resonance, deep-level transient spectroscopy, and doping studies in unalloyed a-Si:H and a-Ge:H; (c) the energies of the dangling-bond states remain constant with respect to the vacuum level for all compositions; (d) the absolute energies of the valence- and conduction-band edges increase and decrease linearly at the same rate between pure a-Si:H and pure a-Ge:H; (e) the position of the Fermi level may be found approximately from the activation energy for conduction.

(5) The band structure constructed according to the scheme outlined in (4) may be exploited to rationalize the observed changes in photoluminescence and photoconductivity in the alloys.

(6) There is strong direct evidence that the poorer photoelectronic properties in the Ge-rich alloys are caused only partly by the band-structure changes outlined in (4), and that a major additional cause is the occurrence of increased heterostructure in the films.

ACKNOWLEDGMENTS

The authors wish to thank Dr. P. B. Kirby and Dr. S. Oguz for fruitful discussions on various aspects of this work. We also thank David MacLeod for technical support, David Lange for the electron microprobe measurements, and Pat Reilly and Maurice Dumais for their assistance with the electron microscopy study. One of us (K.D.M.) has benefited from discussions with Dr. J. M. Gibson of AT&T Bell Laboratories, Murray Hill, New Jersey, on electron microscopy. This work was partially funded by the Solar Energy Research Institute, Golden, Colorado under Subcontract No. XB-2-02144-1 of Prime Contract No. EG-77-C-01-4042 with the Department of Energy.

*Present address: Department of Physics, Zhongshan University, Canton, People's Republic of China.

[1]K. Shirahata and Y. Yukimoto, in *Amorphous Semiconductors, Technologies and Devices,* edited by Y. Hamakama (North-Holland, Amsterdam, 1982), p. 177.

[2]G. Nakamura, K. Sato, and Y. Yukimoto, in *Proceedings of the 16th IEEE Photovoltaic Specialists Conference (San Diego, 1982)* (unpublished), p. 1331.

[3]G. Nakamura, K. Sato, T. Ishihara, M. Usui, K. Okaniwa, and Y. Yukimoto, J. Non-Cryst. Solids **59&60**, 1111 (1983).

[4]Y. Hamakawa, J. Non-Cryst. Solids **59&60**, 1265 (1983).

[5]SERI Technical Reports, November 1981 and May 1982 under SERI Subcontract No. XW-1-9358-1 (unpublished).

[6]S. Z. Weisz, M. Gomez, J. A. Muir, O. Resto, Y. Goldstein, and B. Abeles, Appl. Phys. Lett. **44**, 634 (1984).

[7]Nguyen Van Dong, Tran Hun Danh, and J. Y. Leny, J. Appl. Phys. **52**, 338 (1981).

[8]W. Paul, in *Fundamental Physics of Amorphous Semiconductors,* Vol. 25 of *Springer Series in Solid State Sciences,* edited by F. Yonezawa (Springer, Heidelberg, 1981), p. 72.

[9]B. von Roedern, D. K. Paul, J. Blake, R. W. Collins, G. Moddel, and W. Paul, Phys. Rev. B **25**, 7678 (1982).

[10]D. Hauschildt, R. Fischer, and W. Fuhs, Phys. Status Solidi B **102**, 563 (1980).

[11]J. Bullot, M. Galin, M. Gauthier, and B. Bourdon, J. Phys. (Paris) **44**, 713 (1983). See also L. Chahed, C. Senemaud, M.

L. Thèye, J. Bullot, M. Galin, M. Gauthier, B. Bourdon, and M. Toulemonde, Solid State Commun. **45**, 649 (1983).

[12]K. Nozawa, Y. Yamaguchi, J. Hanna, and I. Shimizu, J. Non-Cryst. Solids **59&60**, 533 (1983).

[13]A. Morimoto, T. Muira, M. Kumeda, and T. Shimizu, J. Appl. Phys. **53**, 7299 (1982).

[14]J. Bullot, M. Gauthier, M. Schmidt, Y. Catherine, and A. Zamouche, Philos. Mag. **B49**, 489 (1984).

[15]A. H. Mahan, D. L. Williamson, and A. Madan, Appl. Phys. Lett. **44**, 220 (1984).

[16]B. von Roedern, A. H. Mahan, R. Könenkamp, D. L. Williamson, A. Sanchez, and A. Madan, J. Non-Cryst. Solids **66**, 13 (1984).

[17]D. K. Paul, B. von Roedern, S. Oguz, J. Blake, and W. Paul, J. Phys. Soc. Jpn. (Suppl. A) **49**, 1261 (1980).

[18]W. Paul, D. K. Paul, B. von Roedern, J. Blake, and S. Oguz, Phys. Rev. Lett. **46**, 1016 (1981).

[19]R. W. Collins and W. Paul, Phys. Rev. B **25**, 5257 (1982).

[20]Deduced from measurements of the space-charge-limited current. See R. L. Weisfield, J. Appl. Phys. **54**, 6401 (1983).

[21]A. Morimoto, T. Miura, M. Kumeda, and T. Shimizu, Jpn. J. Appl. Phys. **20**, L833 (1981).

[22]R. A. Rudder, J. W. Cook, and G. Lucovsky, in *Proceedings of the 17th International Conference on the Physics of Semiconductors (1984)* (unpublished).

[23]The system was designed and constructed at Harvard by B. von Roedern and R. L. Weisfield. A technical description may be found in the SERI Technical Reports of February 1983 and October 1983 under SERI Subcontract No. XB-2-02144-1 (unpublished) and also in Ref. 24.

[24]W. Paul (unpublished).

[25]P. B. Kirby, W. Paul, C. Lee, S. Lin, B. von Roedern, and R. L. Weisfield, Phys. Rev. B **28**, 3635 (1983).

[26]D. E. Carlson and C. R. Wronski, in *Amorphous Semiconductors,* Vol. 36 of *Topics in Applied Physics,* edited by M. H. Brodsky (Springer, Heidelberg, 1979), p. 287.

[27]A. E. Delahoy and R. W. Griffith, J. Appl. Phys. **52**, 6337 (1981).

[28]B. G. Yacobi, R. W. Collins, G. Moddel, P. Viktorovitch, and W. Paul, Phys. Rev. B **24**, 5907 (1981).

[29]Balzers QMG 111B quadrupole residual gas analyzer.

[30]R. R. Corderman and P. E. Vanier, J. Appl. Phys. **54**, 3987 (1983).

[31]R. W. Collins, Ph.D. thesis, Harvard University, 1982.

[32]G. Moddel, D. A. Anderson, and W. Paul, Phys. Rev. B **22**, 1918 (1980).

[33]H. G. Grimmeiss and L. A. Ledebo, J. Appl. Phys. **46**, 2155 (1975).

[34]M. Vaněček, J. Kočka, J. Stuchlík, Z. Kožíšek, O. Šticka, and A. Tříska, Sol. Energy Mater. **8**, 411 (1983); J. Kočka, M. Vaněček, Z. Kožíšek, O. Šticka, and J. Beichler, J. Non-Cryst. Solids **59&60**, 293 (1983).

[35]Alternatively, an estimate of the optical gap, E_g, may be obtained by a linear extrapolation from the data using the relation $(\alpha h\nu)^{1/2}=B(h\nu-E_g)$ (Ref. 36). This formula assumes a constant momentum matrix element for the optical transitions and parabolic densities of states at the valence- and conduction-band edges. Both assumptions are probably incorrect, as inferred from attempts to fit data on $\epsilon_2(\nu)$ using approximately known densities of states derived from photoemission (Ref. 37). As a result, analyses using the above expression (Ref. 38), give values of E_g which depend on the range of α from which extrapolation is performed, or what is the same thing, values of E_g which depend on the thickness of the sample measured. In view of these problems, although the use of an accurate formula from which E_g may be determined is clearly preferable, we shall, for the present, continue to use an empirical definition of energy gap, E_{04}, whose accuracy depends only on accurate experimentation.

[36]J. Tauc, R. Grigorovici, and A. Vancu, Phys. Status Solidi **15**, 627 (1966).

[37]See, for instance, L. Ley, in *The Physics of Hydrogenated Amorphous Silicon II,* Vol. 56, of *Topics in Applied Physics,* edited by J. D. Joannopoulos and G. Lucovsky (Springer, Heidelberg, 1984).

[38]G. D. Cody, B. G. Brooks, and B. Abeles, Sol. Energy Mater. **8**, 231 (1982).

[39]G. A. N. Connell and A. Lewis, Phys. Status Solidi B **60**, 291 (1973). The computer program used to analyze the optical data was written by R. L. Weisfield.

[40]We define the hydrogen content as C_H (at.%)$=100N_H/(N_H+N_{Si}+N_{Ge})$ where N_H, N_{Si}, and N_{Ge} are the atomic concentrations of H, Si, and Ge, respectively. The value for m of 0.62 at.%/eV cm^{-1} used for the a-Si:H samples, was determined by Oguz (Ref. 41), on sputtered a-Si:H from a calibration of the intensity of the Si—H wag modes against C_H determined from nuclear reactions by W. A. Lanford. For the alloys, the value for m of 0.39 at.%/eV cm^{-1} is a median value based on the results of Fang *et al.* (Ref. 42), who studied the hydrogen content of glow discharge a-Ge:H and a-Si:H by ir spectroscopy, gas evolution, and nuclear reaction techniques. The m value of 0.37 at.%/eV cm^{-1} used for the a-Ge:H samples is also based on the same paper.

[41]S. Oguz, Ph.D. thesis, Harvard University, 1981.

[42]C. J. Fang, K. J. Gruntz, L. Ley, M. Cardona, F. J. Demond, G. Müller, and S. Kalbitzer, J. Non-Cryst. Solids **35&36**, 255 (1980).

[43]D. L. Staebler and C. R. Wronski, Appl. Phys. Lett. **31**, 292 (1977).

[44]The 1975- and 2090-cm^{-1} vibrations have often been ascribed to the respective dihydride configurations, Ge-H_2 (Ref. 45) and Si-H_2 (Refs. 46—48). It has been shown that these vibrations can also arise from other contributions (Refs. 49—51), and it is now generally accepted that they cannot be uniquely assigned to dihydrides. Similarly, as suggested from the recent work of Wagner and Beyer on a-Si:H (Ref. 51), the vibrations at 1875 and 2000 cm^{-1} may not be exclusively associated with monohydrides.

[45]D. Bermejo and M. Cardona, J. Non-Cryst. Solids **32**, 421 (1979).

[46]M. H. Brodsky, M. Cardona, and J. J. Cuomo, Phys. Rev. B **16**, 3556 (1977).

[47]P. J. Zanzucchi, C. R. Wronski, and D. E. Carlson, J. Appl. Phys. **48**, 5227 (1977).

[48]G. Lucovsky, R. J. Nemanich, and J. C. Knights, Phys. Rev. B **19**, 2064 (1979).

[49]W. Paul, Solid State Commun. **34**, 283 (1980).

[50]H. Shanks, C. J. Fang, L. Ley, M. Cardona, F. J. Demond, and S. Kalbitzer, Phys. Status Solidi B **100**, 43 (1980).

[51]H. Wagner and W. Beyer, Solid State Commun. **48**, 585 (1983).

[52]G. Lucovsky, in *Fundamental Physics of Amorphous Semiconductors,* Vol. 25 of *Springer Series in Solid State Sciences,* edited by F. Yonezawa (Springer, Heidelberg, 1981), p. 87.

[53]M. A. Paesler, D. A. Anderson, E. C. Freeman, G. Moddel, and W. Paul, Phys. Rev. Lett. **41**, 1492 (1978).

[54]G. Lucovsky (private communication).

[55]G. Lucovsky, J. Yang, S. S. Chao, J. E. Tyler, and W. Czuba-

tyj, Phys. Rev. B **28**, 3225 (1983).
[56]W. Paul, G. A. N. Connell, and R. J. Temkin, Adv. Phys. **22**, 529 (1973).
[57]R. J. Temkin, W. Paul, and G. A. N. Connell, Adv. Phys. **22**, 581 (1973).
[58]G. A. N. Connell, R. J. Temkin, and W. Paul, Adv. Phys. **22**, 643 (1973).
[59]M. Milleville, W. Fuhs, F. J. Demond, H. Mannsperger, G. Müller, and S. Kalbitzer, Appl. Phys. Lett. **34**, 173 (1979); J. Perrin, I. Solomon, B. Bourdon, J. Fontenille, and E. Ligeon, Thin Solid Films **62**, 327 (1979).
[60]See, for instance, Refs. 17 and 18 and also S. Oguz, R. W. Collins, M. A. Paesler, and W. Paul, J. Non-Cryst. Solids **35&36**, 231 (1980); W. Beyer and H. Wagner, *ibid.* **59&60**, 161 (1983).
[61]E. C. Freeman and W. Paul, Phys. Rev. B **20**, 716 (1979).
[62]D. L. Morel and T. D. Moustakas, Appl. Phys. Lett. **39**, 612 (1981).
[63]G. Nakamura, K. Sato, H. Kondo, Y. Yukimoto, and K. Shirahata, J. Phys. (Paris) Colloq. Suppl. 10 **42**, C4-483 (1981).
[64]M. A. Paesler, S. C. Agarwal, S. J. Hudgens, and H. Fritzsche, in *Tetrahedrally Bonded Amorphous Semiconductors (Yorktown Heights), Proceedings of the International Conference on Tetrahedrally Bonded Amorphous Semiconductors,* edited by M. H. Brodsky, S. Kirkpatrick, and D. Weaire (AIP, New York, 1974), p. 37.
[65]G. Moddel, Ph.D. thesis, Harvard University, 1981.
[66]W. Paul (unpublished).
[67]C. Y. Huang, S. Guha, and S. J. Hudgens, J. Non-Cryst. Solids **59&60**, 545 (1983).
[68]C. Senemaud, C. Cardinaud, and G. Villela, Solid State Commun. **50**, 643 (1984).
[69]See Refs. 1, 6, 10, 11, and also J. Chevallier, H. Wieder, A. Onton, and C. R. Guarnieri, Solid State Commun. **24**, 867 (1977), and K. C. Kao, R. D. McLeod, C. H. Leung, H. C. Card, and H. Watanabe, J. Phys. D **16**, 1801 (1983).
[70]M. L. Thèye, in *Amorphous and Liquid Semiconductors,* edited by J. Stuke and W. Brenig (Taylor and Francis, London, 1974), p. 479.
[71]G. A. N. Connell and J. R. Pawlik, Phys. Rev. B **13**, 787 (1976).
[72]R. A. Rudder, J. W. Cook, Jr., and G. Lucovsky, Appl. Phys. Lett. **43**, 871 (1983).
[73]That a linear increase in $y=$(partial pressure of GeH_4)/(total pressure of GeH_4 plus SiH_4) may not be automatically equated to a linear increase in x has been demonstrated by Nozawa *et al.* (Ref. 12), who found that the functional variation of the gap with y depended on the rf power applied to the gas mixture. See also Ref. 1.
[74]W. Paul, in *Amorphous Semiconductors (Nathiagali, Pakistan, 1978), Proceedings of the Third International Summer College on Physics and Contemporary Needs* (Plenum, New York, 1979).
[75]See, for instance, H. Dersch, J. Stuke, and J. Beichler, Phys. Status Solidi B **105**, 265 (1981); W. B. Jackson, Solid State Commun. **44**, 477 (1982).
[76]M. Stutzmann, J. Stuke, and H. Dersch, Phys. Status Solidi B **115**, 141 (1983).
[77]This energy difference is the subject of much current measurement and disagreement. Some deep-level transient spectroscopy (DLTS) measurements suggest 1.25 eV (Ref. 78), others 0.9 eV (Ref. 79). An analysis of spectroscopic data has given 1.3 eV (Ref. 80). Our measurements (Ref. 25) of the electron and hole lifetime changes with shift of the Fermi level showed a factor of about 100 change in both when $(E_c-E_F)_0$ was changed from 0.95 to 0.67 eV and tentatively placed the D^- energy inside this range. However, more complete measurements of lifetimes versus Fermi-level position by Spear *et al.* (Ref. 81), conclude that the D^0 state lies 0.95 eV below E_c. It should be noted that there are many complicating factors involved in defining the appropriate energy scale for the different types of measurement and adjusting the scale to any desired temperature. Our choice of 1.0 eV is based partly on our conclusion (see text) that the present results are less compatible with the higher values.
[78]D. V. Lang, J. D. Cohen, and J. P. Harbison, Phys. Rev. B **25**, 5258 (1982); J. D. Cohen, J. P. Harbison, and K. W. Wecht, Phys. Rev. Lett. **48**, 109 (1982).
[79]H. Okushi, T. Takahama, Y. Tokumaru, S. Yamasaki, H. Oheda, and K. Tanaka, Phys. Rev. B **27**, 5184 (1983).
[80]W. B. Jackson and N. M. Amer, Phys. Rev. B **25**, 5559 (1982), and also see the paper by Jackson in Ref. 75.
[81]W. E. Spear, H. L. Steemers, P. G. LeComber, and R. A. Gibson, Philos. Mag. **B50**, L33 (1984).
[82]Approximately at midgap and reasonably consistent with estimates of Stutzmann *et al.* (Ref. 76).
[83]Dr. F. Evangelisti has informed us that he has concluded that E_v in Ge is higher than E_v in Si by 0.3 ± 0.1 eV, which fits our indirect arguments.
[84]W. Paul and D. A. Anderson, Sol. Energy Mater. **5**, 229 (1981).
[85]This mode was first assigned to SiH_2 entities (Refs. 46–48), but it is increasingly accepted (Refs. 49–51) that, since absorption at this frequency is found in the absence of bending modes near 800–900 cm^{-1}, monohydride in as yet unidentified surroundings may be responsible. Whether the absorption is caused by $Si-H_2$ or Si-H in this or other environments is less relevant here than the empirical correlation with inhomogeneity.
[86]J. C. Knights, R. A. Lujan, M. P. Rosenblum, R. A. Street, D. K. Biegelsen, and J. A. Reimer, Appl. Phys. **52**, 5329 (1981).
[87]R. C. Ross and R. Messier, J. Appl. Phys. **52**, 5329 (1981).
[88]R. C. Ross, A. G. Johncock, and A. R. Chan, J. Non-Cryst. Solids **66**, 81 (1984).
[89]See, D. A. Anderson and W. Paul, Philos. Mag. **B44**, 187 (1981) or W. Paul and D. A. Anderson, Sol. Energy Mater. **5**, 229 (1981) for illustration and earlier references.
[90]See Ref. 89 and also D. A. Anderson and W. Paul, J. Phys. Soc. Jpn. Suppl. A **49**, 1197 (1980).
[91]J. C. Knights and R. A. Lujan, Appl. Phys. Lett. **35**, 244 (1979).
[92]H. Overhof and W. Beyer, J. Non-Cryst. Solids **35&36**, 375 (1980).

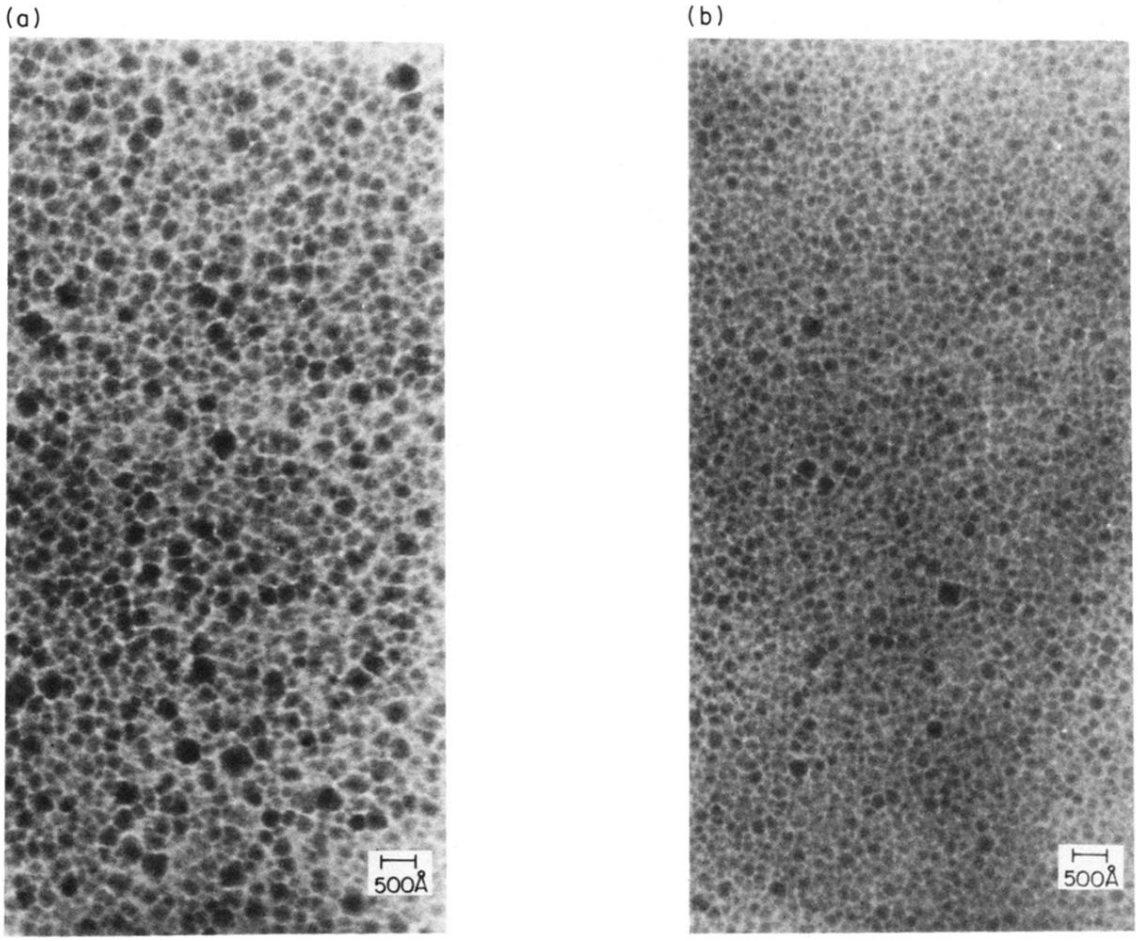

FIG. 13. Bright field TEM images of a-$Si_{0.5}Ge_{0.5}$:H prepared at (a) 230 °C and (b) 300 °C.